Available online at www.sciencedirect.com
SCIENCE DIRECT®
Advances in Space Research 33 (2004) 381–385
ADVANCES IN SPACE RESEARCH (a COSPAR publication)
www.elsevier.com/locate/asr

Shock–cloud interactions in the Vela SNR: preliminary results of an XMM-Newton observation

F. Bocchino [a,*], M. Miceli [b], A. Maggio [a]

[a] Instituto Nazionale di Astrofisica – Osservatorio Astronomico di Palermo, 90134 Palermo, Italy
[b] Dipartimento di Scienze Fisiche ed Astronomiche, Università di Palermo, Italy

Received 3 December 2002; received in revised form 17 July 2003; accepted 6 August 2003

Abstract

The study of the clumpy and irregular features in the X-ray emission of middle-aged supernova remnants shells allows us to shed light on the various characteristic of the interstellar medium, like its structure and composition. We have observed with XMM-Newton a small knot in the Vela SNR, which previous ROSAT studies have indicated as one of the best examples of an interaction between the SNR shock and an isolated cloud. We present preliminary results of this study. Thanks to the combination of good spectral and spatial resolution of the EPIC camera, we have realized maps of the X-ray emission in three different bands, pinpointing the contribution from different spatial regions. We have also studied the relation between the mean photon energy in a 10 arcsec/pixel image and the pixel count rate, arguing that at least two kinds of isobaric structures (a small isolated cloud and a larger feature) can be identified, both of which have interacted with a shock and both with their own thermal structure.

Keywords: X-rays: ISM; ISM: supernova remnants; ISM: structure; ISM: individual objects; Vela supernova remnant; ISM: clouds

1. The study of shell SNR shock regions

High spatial and spectral resolution X-ray and optical observations of supernova remnants (SNRs) offer a unique opportunity to study the interaction of interstellar shocks with the local environment, and then to get crucial information on the structure of the interstellar medium (ISM). The gross mechanism responsible for the X-ray and optical emission of the middle-aged SNRs is well-understood: optical filaments arise from slow radiative shocks propagating in a dense and cool environment (typical density and temperature values are $n \gtrsim 1$ cm^{-3} and $T \lesssim 10^5$ K), whereas, X-ray emission originates from zones with higher temperature ($T > 10^5$ K) and lower density (usually <1 cm^{-3}). However, the proper interpretation of what we see in high spatial resolution observations is still not straightforward, essentially because the presence of clumps in the ISM disrupts the idealized spherical symmetry of the supernova explosion and its remnant, and determines local variations of the thermodynamical parameters.

In this perspective multi-wavelength observations of SNRs shock regions (e.g., Graham et al., 1995 on Cygnus Loop, or Bocchino et al., 2000 on Vela) may be quite a powerful tool to clarify the relevant physical scenario, but, if the X-ray observations lack sufficient high spatial resolution, they can be subject to several interpretations.

The first scenario points out the importance of evaporation of ISM cloudlets engulfed by the main blast wave. The evaporation is caused by thermal conduction between the cooler cloud and the hotter intercloud medium (ICM) behind the shock. This model typically requires the clouds to be rather small, and this yields practical constraints on cloud filling factors and the small scale structure of the ISM. The evaporative model has been applied in the past to observation of SNRs (Charles et al., 1985; Fesen et al., 1982), and more recently to describe the composite SNR G327.1-1.1 (Bocchino and Bandiera, 2003), but a rigorous comparison between the data and the model, including effects like

* Corresponding author. Tel.: +39-091-233444; fax: +39-91-233444.
E-mail address: bocchino@astropa.unipa.it (F. Bocchino).

0273-1177/$30 © 2003 COSPAR. Published by Elsevier Ltd. All rights reserved.
doi:10.1016/j.asr.2003.08.016

saturated conduction and non-equilibrium of ionization is still lacking.

The second interpretation, based on cloud "bow-shocks", invokes a complete different scenario which emphasizes the role of the overpressured regions in the post-shock flows. Detailed hydrodynamical calculations of shock–cloud interactions show that a reverse reflected shock in the intercloud medium develops as a consequence of the cloud density contrast (see e.g., Stone and Norman, 1992). The reverse shock may eventually become a standing shock, but in any case the pressure and the density of the ICM are raised near the cloud. Recently, Levenson et al. (2002) have invoked the bow-shock scenario to explain a Chandra observation of a portion of the Cygnus Loop shell.

A third interpretation is based on the propagation of a transmitted shock inside an ISM cloud overrun by the primary blast wave. These shocks, whose presence is confirmed by numerical simulations, can be strong enough to produce X-ray emission, especially if the cloud contrast is low and/or the primary shock is fast. Bocchino et al. (2000) have identified two regions in the Vela SNR in which the main blast wave seems to interact with a small isolated cloud and with a cavity wall. These observations are consistent with a model which associates the X-ray emission to secondary shocks in clouds. However, the limited spatial and spectral resolution of the ROSAT PSPC did not allow us to study the region at higher resolution to exclude other scenarios, nor to investigate other potentially relevant effect like the metal depletion of the ISM and to carry out a multi-component spectral analysis, including non-equilibrium of ionization (NEI) effects.

It is clear that these kind of studies have been hampered by the instrumental performances of past-generation X-ray satellites, since many different processes may occur at the same time in the same object and low spatial resolution observation are affected by superposition effects. In fact, the size of the dishomogeneities in the ISM may range between 10^{-3} and 1 parsec ($0.2''d_{\rm kpc}$ and $3.4'd_{\rm kpc}$, respectively, where $d_{\rm kpc}$ is the distance in kpc units). Several hydrodynamical simulations of shocks impinging on a 1 pc cloud show that spectral variations are expected on scales of $\sim$0.1 pc ($\sim 20''d_{\rm kpc}$), and optical observations show that filaments have sub-arcminute spatial structures. As more and more high resolution Chandra and XMM-Newton data become available, this research area is going to have a boost, thanks to the improved spatial and spectral performance of these X-ray observatories.

2. The Vela SNR

The Vela SNR is the nearest object of its kind, located at a distance of $\sim$250 pc (Bocchino et al., 1999; Cha et al., 1999). Moreover, the association with the pulsar PSR B0833-45, which is by now firmly established, indicates that the Vela SNR is rather old. In fact, the characteristic age of PSR B0833-45 is $\sim$11.2 kyr. For these reasons, the Vela SNR is a privileged laboratory for the study of the interaction between the shell and the environment at a very small angular scale; each arcmin correspond to only 0.08 pc at the distance of the remnant.

In particular, the North Rim of the Vela SNR has all the prototypical features of an X-ray shell expanding in a complex environment, as pointed out in several works (Bocchino et al., 1994, 1997, 1999, 2000). Two observations carried out with the ROSAT satellite in the 0.1–2.4 keV band have allowed us to isolate a weak background emission coming from a region not yet shocked by the blast-wave, a region with low X-ray surface brightness, and several regions with strong X-ray enhancements, both at large ($\sim$1°) and small (few arcmin) spatial scales. The same ROSAT analysis has shown that the brightest diffuse regions are characterized by an increased contribution to the total X-ray emission of a soft ($kT = 0.1$ keV) and dense (~ 0.5 cm^{-3}) component that permeates all the North Rim. This observational evidence has been associated to the expansion of slow shocks inside large scale ISM inhomogeneities (e.g., a cavity wall blown by progenitor wind), but other scenarios like clouds evaporation and bow shocks cannot be excluded. Interestingly, the smallest X-ray clump in the North Rim, introduced as Fil D in Bocchino et al. (1999), does not show a filling factor increment and presents clear indication of higher density of the cool thermal component with respect to adjacent regions.

Several issues were left open by the ROSAT results, and in particular, the presence of NEI in both the thermal components, the ultimate origin if Fil D and its relation with the environment, the characterization of the low surface brightness regions. Moreover, it was not possible to estimate the metal abundances.

3. The XMM-Newton observation

The region around Fil D (RA = 08:35:35, DEC = −42:54:00, J2000) was observed by XMM-Newton on November 9th 2001. After having screened out intervals with high proton background, the exposure times are 12.4 ks for PN and 26.0 ks for MOS. The X-ray emission of the region in two different bands is shown in Fig. 1.

There are striking differences in the morphology of the X-ray emission in the two bands. It is important to note that the Fil D complex is well visible in the softer band, where it is the most important feature in the image, while it is barely visible in the higher band, where other larger features appear.

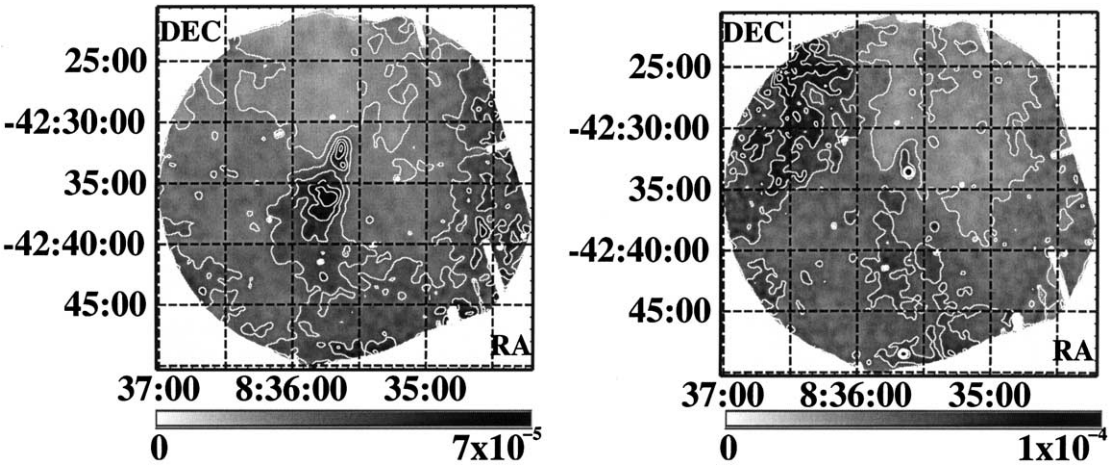

Fig. 1. Count rate images (MOS1 equivalent) centered on the region of Fil D, in the 0.3–0.5 keV band (left) and 0.5–1 keV band (right). The images are obtained a weighted sum of the PN, MOS1 and MOS2 images, and are vignetting corrected. Seven contour levels, equispaced between 0% and 100% of the peak value (7×10^{-5} and 10^{-4} cnt s^{-1} $pixel^{-1}$, respectively, 4 arcsec/pixel) are shown.

On the contrary, the emission above 1 keV is characterized by a set of point sources of unknown origin, and the extended emission from the Vela SNR is absent. A comparison of the log N–log S function computed in this field and the same function computed in a set of XMM-Newton pointings of the Galactic Plane reveal that in our Vela XMM-Newton field there is an excess of weak sources (<0.01 cnt s^{-1}) and a lack of brighter source. More work is being performed on this topic.

4. The thermal conditions of the region

The patchy morphology of the X-ray emission in this region suggests that the expansion is occurring in a complex environment. Under these circumstances we expect the coexistence of different thermal conditions due to the different physical effects generated by the impact of the shock on a variety of ISM inhomogeneities. It is therefore, of primary importance to quantify the spatial distribution of the thermal parameters, in order to understand which is the ultimate origin of the emission.

As a first step in the analysis of this data, we have concentrated ourselves on two parameters and their relation: the mean photon energy ($\bar{E}$ hereafter) in a given pixel of the image, and its count rate. It is intuitive that in the case of different regions with the same pressure but different temperatures, higher $\bar{E}$ corresponds to a lower count-rate. This kind of region may be very common in middle-aged supernova remnants expanding in inhomogeneous medium, and several authors have pointed out the multi-temperature structure of the Vela SNR (Bocchino et al., 1999; Lu and Aschenbach, 2000). However, the lack of high $\bar{E}$ – low rate correspondence does not necessarily imply pressure gradient, as the mass of the emitting plasma also enters in the determination of the count rate.

The mean photon energy has been computed with a spatial binning of 10 arcsec/pixel, in order to have at least 10 photons each pixel, and is reported in Fig. 2, along with the count-rate in the EPIC band (0.3–10 keV). While it is apparent that the bright Fil D complex has the lowest $\bar{E}$, this is not true for the equally brighter North-East (NE) region, thus suggesting that either pressure equilibrium is not achieved or that volume (or mass) effects are at work.

As a powerful diagnostic tool, we have used the scatter plot $\bar{E}$-pixel count rate, displayed for all pixels in Fig. 3, in which we have also traced the expected behavior for an isobaric plasma with temperature gradient, and other potentially interesting behaviors, like an isothermal plasma with a pressure (or volume) gradient. This plot shows that some isobaric trends are apparent (like the lower and upper envelope to the distribution of points), but that the hypothesis of an isobaric plasma for all the field of view must be rejected.

Fig. 4 shows the $\bar{E}$-rate scatter plot for two selected regions, that is the brightest portion of Fil D and the adjacent low surface brightness region (A and B). These two regions clearly identify an isobaric line in the $\bar{E}$-rate plot, thus indicating that not only Fil D, but also the surrounding fainter regions are part of a single structure with different temperature but in pressure equilibrium.

It is interesting to explore the $\bar{E}$-rate relation of other regions. Fig. 5 shows the relation for the NE bright region (C) and the fainter large region next to it (D). These two regions also show an overall isobaric behavior, with a $\bar{E}$ range (and therefore probably a temperature range) slightly higher than the Fil D region. However, it is important to note that the points related to the NE and North (N) region do not overlap with the points of Fil D, and this implies that either the value of the pressure is larger than in Fil D or the volume or the mass of the emitting plasma is higher than in Fil D.

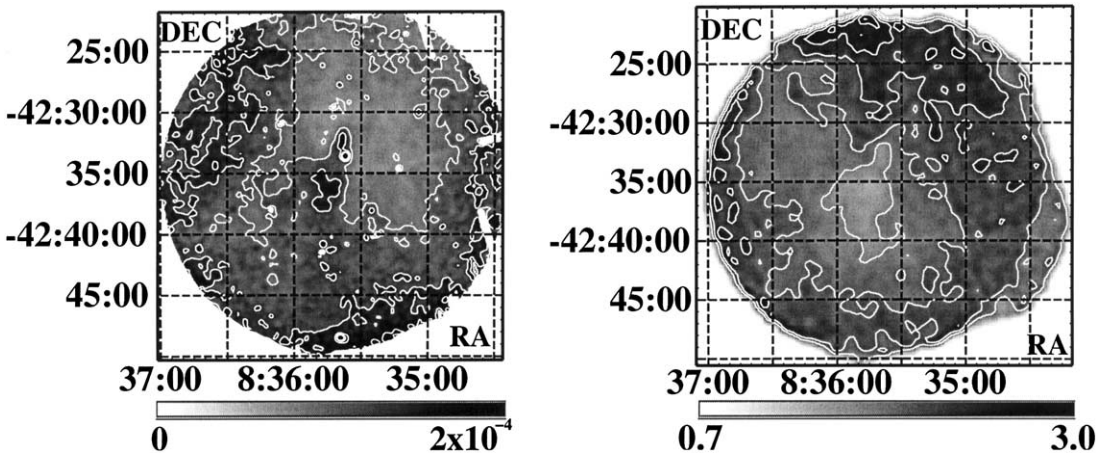

Fig. 2. Map of the count rate in the 0.3–10 keV (vignetting corrected, PN + MOS, left panel, 8 contour levels equispaced between 0 and the maximum at 1.85×10^{-4} cnt s^{-1} $pixel^{-1}$) and map of the mean photon energy ($\bar{E}$, right panel; black is 0.7 keV, white is 3 keV, contours levels are 630, 944, 1258, 1572, 1886 and 2200 eV).

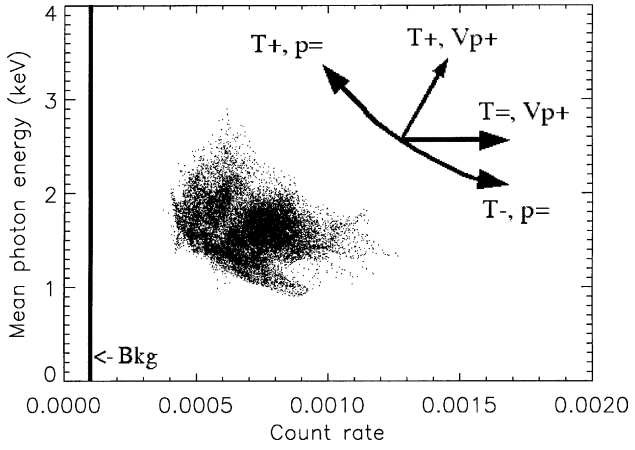

Fig. 3. $\bar{E}$ – countrate scatter plot for all the pixels of the image in Fig. 2. We have also indicated the estimated background value and the expected isobaric and isothermal trends in the plot (T is temperature, V is volume, p is pressure,"+" is increasing and "−" is decreasing).

The region south of Fil D (figures not reported) shows a behavior more similar to the N–NE region, thus confirming the uniqueness of the bright Fil D region with respect of its environment.

5. Discussion and conclusions

As a first step in our analysis of a region in the NE rim of Vela SNR, we have used broad band photometry and the mean photon energy vs. rate diagram to isolate potentially interesting regions. This diagram is an especially useful tool, exploiting at the same time the high XMM-Newton throughput, and the instrumental spatial and spectral response. While the diagram does not convey the detailed information of a spectral fitting, it is of great importance to identify regions in different thermal regimes, which will be the subject of the forthcoming spectral analysis.

Unfortunately, pressure variations and mass (or volume) variations cannot be disentangled on the basis of the $\bar{E}$-rate diagram alone. Additional information from the spectra (for instance the non-equilibrium of ionization time τ) is required, and we are working on this topic.

The most obvious explanation we have found for the different behavior of the central and bright Fil D with respect of its surroundings is a different extension along the line of sight of the emitting plasma. Fil D has a small

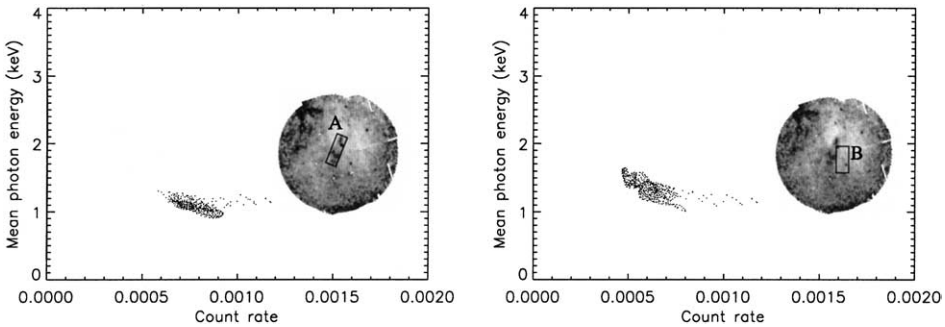

Fig. 4. $\bar{E}$ – countrate scatter plot for two selected regions in the field of view (A and B, showed in the insets).

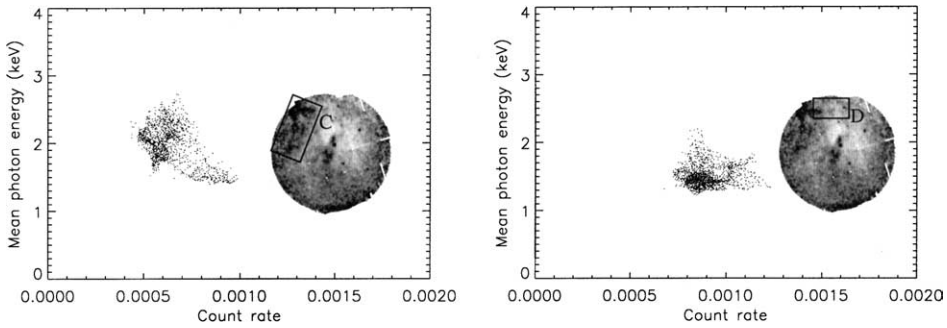

Fig. 5. Same as previous figure but for the NE and N regions (C and D).

extension, because its isobaric curve lies below the one of the other regions, thus suggesting an origin in terms of an isolated small (∼0.2 pc) feature, probably a small ISM cloud, which, however, has its own density distribution and therefore shows a range of temperatures (Fig. 4).

On the other hand, the N–NE region and the South region are physically distinct from Fil D, and show an higher emitting mass, implying, according our opinion, a larger extension of the emitting plasma along the line of sight. This component, which also shows a range of temperatures, is may be associated to larger inhomogeneities like large clouds, again with density variation within it, and which also has been impacted by a shock.

Additional work is being performed on this data. In particular, spectral analysis of region selected on the basis of these findings will allow us to verify this interpretation and to further constrain our model.

References

Bocchino, F., Bandiera, R. BeppoSAX observation of the composite remnant G327.1-1.1. Astron. Astrophys. 398, 195–202, 2003.

Bocchino, F., Maggio, A., Sciortino, S. ROSAT PSPC observation of the northeast region of the Vela supernova remnant. 1: evidence of thermal structure on a scale of 5 min. Astrophys. J. 437, 209–221, 1994.

Bocchino, F., Maggio, A., Sciortino, S. ROSAT PSPC observation of the Northeast region of the Vela supernova remnant. II. Spectral analysis with a nonequilibrium of ionization emission model. Astrophys. J. 481, 872–882, 1997.

Bocchino, F., Maggio, A., Sciortino, S. ROSAT PSPC observation of the NE region of the Vela supernova remnant. III. The two-component nature of the X-ray emission and its implications on the ISM. Astron. Astrophys. 342, 839–853, 1999.

Bocchino, R., Maggio, A., Sciortino, S., et al. Multi-wavelength observations and modelling of shock–cloud interaction regions in the Vela supernova remnant. Astron. Astrophys. 359, 316–336, 2000.

Cha, A.N., Sembach, K.R., Danks, A.C. The distance to the Vela supernova remnant. Astrophys. J. 515, L25–L28, 1999.

Charles, P.A., Kahn, S.M., McKee, C.F. Einstein observations of selected regions of the Cygnus Loop. Astrophys. J. 295, 456–462, 1985.

Fesen, R.A., Blair, W.P., Kirshner, R.P. Spectrophotometry of the Cygnus Loop. Astrophys. J. 262, 171–188, 1982.

Graham, J.R., Levenson, N.A., Hester, J.J., et al. An X-ray and optical study of the interaction of the Cygnus Loop supernova remnant with an interstellar cloud. Astrophys. J. 444, 787–795, 1995.

Levenson, N.A., Graham, J.R., Walters, J.L. Shell shock and cloud shock: results from spatially resolved X-Ray spectroscopy with Chandra in the Cygnus Loop. Astrophys. J. 576, 798–805, 2002.

Lu, F.J., Aschenbach, B. Spatially resolved X-ray spectroscopy of the Vela supernova remnant. Astron. Astrophys. 362, 1083–1092, 2000.

Stone, J.M., Norman, M.L. The three-dimensional interaction of a supernova remnant with an interstellar cloud. Astrophys. J. 390, L17–L19, 1992.